

A simple model for dynamic heterogeneity in glass-forming liquids

Rajib K Pandit* and Horacio E. Castillo†

Department of Physics and Astronomy and Nanoscale and Quantum Phenomena Institute, Ohio University, Athens, Ohio 45701, USA

(Dated: October 24, 2023)

Liquids near the glass transition exhibit dynamical heterogeneity, i.e. local relaxation rates fluctuate strongly over space and time. Here we introduce a simple continuum model that allows for quantitative predictions for the correlators describing these fluctuations. We find remarkable agreement of the model predictions for the dynamic susceptibility $\chi_4(t)$ with numerical results for a binary hard-sphere liquid and for a Kob-Andersen Lennard-Jones mixture. Under this model, the lifetime τ_{ex} of the heterogeneities has little effect on the position $t = t_4 \sim \tau_\alpha$ of the peak of $\chi_4(t)$, but it controls the decay of $\chi_4(t)$ after the peak, and we show how to estimate it from this decay.

Introduction. When cooled or compressed fast enough, most liquids will undergo a glass transition, where the characteristic timescale for relaxation, the α -relaxation time τ_α [1–3] grows smoothly but extremely rapidly. Together with the increase in relaxation time, *dynamical heterogeneity* emerges: relaxation becomes much slower in some regions than in others [2, 4–6]. In this work we introduce a phenomenological model for dynamic heterogeneity which is directly based on this intuitive description and uses a local relaxation rate $\gamma(\vec{r}, t) \equiv 1/\tau_{\vec{r}}(t)$ as its basic variable. The model allows to write the multi-point correlators measured in numerical simulations in terms of the two-point correlator $s(\vec{q}, t, t')$ of $\gamma(\vec{r}, t)$, which has a direct interpretation in terms of the size and lifetime of the heterogeneous regions. These quantities can provide a more direct connection between numerical simulation results and the results of experiments [4, 6–8] on dynamical heterogeneity. More immediately, we show in this work that: (i) numerical simulation data for two glass-forming systems [9, 10] are consistent with predictions from the model; (ii) the model explains quantitatively and in a transparent way some of the general features [11] of the numerical results, and (iii) the model provides a new, simpler way to extract an estimate of the lifetime of the heterogeneities from numerical simulation data.

Probing relaxation in numerical simulations requires detecting changes in individual particle positions or orientations over a certain time interval of length t , i.e. measuring a two-time observable $C(t)$ [5]. For example the overlap $C(t) = F_o(t)$ [9] gives the fraction of “slow particles”, i.e. those particles that over the interval t have had displacements shorter than a certain distance a . Because of dynamic heterogeneity, the fraction of slow particles varies over space and time. This variation can be probed by measuring four-point functions such as the *four-point structure factor* $S_4(\vec{q}, t)$ [11–13], which is the Fourier-space correlation function of the *local density of slow particles*, or, equivalently, the structure factor of the slow particles, (up to a trivial additive constant). The limit $\chi_4(t) = \lim_{q \rightarrow 0} S_4(\vec{q}, t)$ [9, 11, 13–15], called the *dynamic susceptibility*, captures contributions from dynamic

heterogeneities of all spatial extents, and has been a central quantity in numerical studies of dynamical heterogeneity, where it has been often used to provide an overall measure of the degree of heterogeneity, or, in other words, of the intensity of the fluctuations. Although there have been some efforts to predict or interpret the time dependence of the four-point dynamic susceptibility $\chi_4(t)$, particularly for times up to the α -relaxation time [14], much less is known about it for times $t > \tau_\alpha$, and about how the time evolution of $\chi_4(t)$ is connected with the time evolution of the heterogeneous regions.

Observables and data. For simplicity, we consider only systems, such as supercooled liquids, where (i) the heterogeneity is dynamic, not static, and therefore all thermodynamic averages are translation invariant, and (ii) the dynamics is time-translation-invariant (TTI), e.g. aging is not present. We also restrict ourselves to observables involving only one time interval from time 0 to time t . We probe the dynamics by using the microscopic overlap function $w_n(t) = \theta[a - |\vec{r}_n(t) - \vec{r}_n(0)|]$, where $\theta(x)$ is the Heaviside step function, $\vec{r}_n(t), n = 1, \dots, N$ is the position of the n -th particle at time t , and a is a characteristic distance that is larger than the typical amplitude of vibrational motion. We introduce the local relaxation function $C_{\vec{r}}(t)$,

$$C_{\vec{r}}(t) \equiv \rho^{-1} \sum_{n=1}^N w_n(t) \delta(\vec{r}_n(0) - \vec{r}), \text{ with } \langle C_{\vec{r}}(t) \rangle = C(t), \quad (1)$$

where ρ is the average particle density, $\langle \dots \rangle$ is an average over thermal fluctuations, and $C(t)$ is the global two-point correlator, i.e. the average overlap $C(t) = F_o(t) \equiv N^{-1} \sum_{n=1}^N \langle w_n(t) \rangle$ [9]. Fluctuations are characterized by the four-point dynamic structure factor $S_4(\vec{q}, t)$ [11, 12],

$$S_4(\vec{q}, t) \equiv \rho^2 N^{-1} \int d^d r e^{-i\vec{q} \cdot \vec{r}} \langle [C_{\vec{r}}(t) - C(t)][C_{\vec{0}}(t) - C(t)] \rangle \quad (2)$$

$$= N^{-1} \sum_{n, n'=1}^N \left\langle w_n(t) w_{n'}(t) e^{i\vec{q} \cdot (\vec{r}_n(0) - \vec{r}_{n'}(0))} \right\rangle - \delta_{\vec{q}, 0} N C^2(t). \quad (3)$$

Numerical results [16, 17] are discussed for a 3D hard-sphere binary mixture (HARD) [9], and for a 3D Kob-Andersen Lennard-Jones binary mixture (KALJ) [10].

Continuum model for dynamic heterogeneity. The model we introduce focuses on the α -relaxation regime, i.e. times t during the second step in the two-step relaxation. It is based on two assumptions, which we discuss below.

*Present address: Exact Sciences, Redwood City, 94063 CA, USA

Motivation for Assumption 1 Even though four-point functions were introduced to describe the collective phenomenon of dynamic heterogeneity, they capture much more than that. In Ref. [18] it was shown that at very long times t , the collective contributions to the four-point function $S_4(\vec{q}, t)$ are negligible compared to the single-particle, spatially uncorrelated, \vec{q} -independent contribution $S_4^{\text{sp}}(\vec{q}, t) = \chi_4^{\text{sp}}(t) \approx C(t) - C^2(t)$. To reproduce this behavior, we introduce:

Assumption 1 The local relaxation function $C_{\vec{r}}(t)$ is the sum of two mutually independent random variables, the collective part $C_{\vec{r}}^{\text{coll}}(t)$ and the single particle part $C_{\vec{r}}^{\text{sp}}(t)$,

$$C_{\vec{r}}(t) = C_{\vec{r}}^{\text{coll}}(t) + C_{\vec{r}}^{\text{sp}}(t), \quad \text{with} \quad (4)$$

$$\langle C_{\vec{r}}^{\text{coll}}(t) \rangle = C(t) \quad \text{and} \quad \langle C_{\vec{r}}^{\text{sp}}(t) \rangle = 0. \quad (5)$$

We interpret all correlations between different particles as ‘‘collective’’, thus the single particle part $C_{\vec{r}}^{\text{sp}}(t)$ is spatially uncorrelated at equal times,

$$C_{\vec{r}}^{\text{sp}}(\vec{r}, t) \equiv \rho \langle C_{\vec{r}}^{\text{sp}}(t) C_{\vec{0}}^{\text{sp}}(t) \rangle \propto \delta(\vec{r}), \quad \text{and} \quad S_4^{\text{sp}}(\vec{q}, t) = \chi_4^{\text{sp}}(t). \quad (6)$$

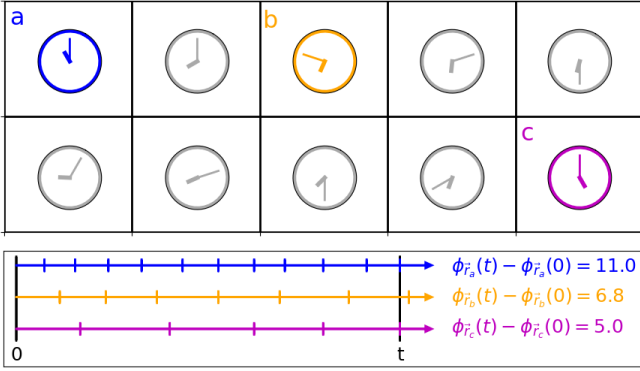


FIG. 1: Converting the idea of space and time dependent relaxation times $\tau_{\vec{r}}(t)$ into the idea of a ‘‘local clock’’. For each region in the system there is an individual local clock $\phi_{\vec{r}}(t)$ (Eq. 7) that counts how many local relaxation times have elapsed up to time t . Each tick mark on a horizontal line represents one relaxation time. For example, of the three highlighted regions, a , b and c , region c has relaxed the slowest, with $\Delta\phi_{\vec{r}_c}(t) = \phi_{\vec{r}_c}(t) - \phi_{\vec{r}_c}(0) = 5.0$ relaxation times elapsed between time 0 and time t . Regions a and b have relaxed generally faster, so the corresponding numbers of elapsed relaxation times between times 0 and t are larger, in this case $\Delta\phi_{\vec{r}_a}(t) = 11.0$.

Motivation for Assumption 2 Dynamic heterogeneity has been described as involving relaxation times differing in different spatial regions [4, 6, 7], i.e. some regions being ‘‘fast’’ and others being ‘‘slow’’. Our model directly translates this intuitive description into quantitative predictions by defining a ‘‘local clock’’ $\phi_{\vec{r}}(t)$ (Fig. 1), which instead of counting in units of seconds, counts in units of the local relaxation time $\tau_{\vec{r}}(t)$,

$$\phi_{\vec{r}}(t) \equiv \int^t dt' / \tau_{\vec{r}}(t'). \quad (7)$$

Thus $\Delta\phi_{\vec{r}}(t) \equiv \phi_{\vec{r}}(t) - \phi_{\vec{r}}(0)$ represents the number of relaxation times elapsed between times 0 and t in the region around

\vec{r} (Fig. 1). Naively one could expect $C_{\vec{r}}^{\text{coll}}(t)$ to depend only on $\Delta\phi_{\vec{r}}(t)$, i.e. $C_{\vec{r}}^{\text{coll}}(t) = \mathcal{C}[\Delta\phi_{\vec{r}}(t)]$ [19–21]. Here $\mathcal{C}(x)$ doesn’t fluctuate, it is a fixed monotonous decreasing function, with $\mathcal{C}(1) = e^{-1} \mathcal{C}(0)$, that represents the shape of the local relaxation function, for example $\mathcal{C}(x) = f_0 \exp(-x)$ for simple exponential relaxation. This *ansatz*, however, does not reproduce $S_4(\vec{q}, t)$, because spatial density fluctuations in the initial state of the system provide two \vec{q} -dependent contributions [18] to $S_4(\vec{q}, t)$. One is $S_4^{\text{st}}(\vec{q}, t) = C^2(t)S(\vec{q})$ (for $q \neq 0$), where $S(\vec{q})$ is the static structure factor; the other, S_4^{mc} [16] was neglected in the case of $\chi_4(t) = \lim_{q \rightarrow 0} S_4(\vec{q}, t)$. This motivates multiplying $\mathcal{C}[\Delta\phi_{\vec{r}}(t)]$ by the initial local particle density $\rho(\vec{r}, 0)$, which leads to:

Assumption 2 The collective contribution is

$$C_{\vec{r}}^{\text{coll}}(t) = \rho^{-1} \rho(\vec{r}, 0) \mathcal{C}[\phi_{\vec{r}}(t) - \phi_{\vec{r}}(0)], \quad (8)$$

$$\text{where} \quad \partial\phi_{\vec{r}}(t)/\partial t \equiv 1/\tau_{\vec{r}}(t) = \gamma(\vec{r}, t) \quad (9)$$

is the local relaxation rate. For simplicity, we assume that $\rho(\vec{r}, t_1)$ and $\phi_{\vec{r}}(t_2)$ are mutually independent random variables, for arbitrary positions \vec{r}, \vec{r}' , and times t_1, t_2 , and that they are smooth and slowly varying in space and time.

Motivation for the definition of τ_{ex} The exchange time τ_{ex} has been defined as the characteristic time for a ‘‘fast’’ region becoming ‘‘slow’’ or viceversa [4, 6, 7]. This translates directly into defining it as the characteristic time for the auto-correlation function of the relaxation rate $\gamma(\vec{r}, t) = 1/\tau_{\vec{r}}(t)$.

Definition of the exchange time τ_{ex}

$$\tau_{\text{ex}} \equiv \frac{\int_0^\infty t \chi_2^\phi(t) dt}{\int_0^\infty \chi_2^\phi(t) dt}, \quad \text{where} \quad \chi_2^\phi(t) \equiv \lim_{q \rightarrow 0} s(\vec{q}, t), \quad (10)$$

$$\text{and} \quad s(\vec{q}, t) \equiv V^{-1} \int d^d r e^{-i\vec{q}\cdot\vec{r}} \langle \delta\gamma(\vec{r}, t) \delta\gamma(\vec{0}, 0) \rangle. \quad (11)$$

Here $\chi_2^\phi(t)$ and $s(\vec{q}, t)$ are two-point functions of the fluctuations $\delta\gamma(\vec{r}, t) \equiv \gamma(\vec{r}, t) - \langle \gamma(\vec{r}, t) \rangle$ of the relaxation rate. The limit $q \rightarrow 0$ in Eq. (10) includes fluctuations at all spatial lengthscales, as in the definition of $\chi_4(t)$ [9, 11, 13–15].

Results: Prediction for the dynamic susceptibility $\chi_4(t)$ By Taylor expanding Eq. (8) up to quadratic order in $\delta\gamma$, Assumptions 1 and 2 lead to

$$\mathcal{C}'(t/\tau) \approx \tau \dot{C}(t), \quad \text{where} \quad C(\tau) = e^{-1}, \quad \text{and} \quad (12)$$

$$\chi_4(t) \equiv \lim_{q \rightarrow 0} S_4(\vec{q}, t) = \dot{C}^2(t) \tilde{\chi}_4^\phi(t) + \chi_{4,b}^{(0)}(t), \quad \text{with} \quad (13)$$

$$\chi_{4,b}^{(0)}(t) \equiv C(t) + [N^{-1} \langle (\delta N)^2 \rangle - 1] C^2(t) \quad (14)$$

representing a background due to single particle and initial density fluctuations.

Eq. (13) is the main result of this work. The factor $\dot{C}^2(t)$ comes directly from the linear term in the Taylor expansion, and its presence is unavoidable for any *ansatz* that contains a factor like $\mathcal{C}[\phi_{\vec{r}}(t) - \phi_{\vec{r}}(0)]$ that attempts to represent the effects of fluctuating local relaxation rates. The factor $\tilde{\chi}_4^\phi(t)$ [22] is predicted to be a positive monotonously increasing function of t , which has no special feature for $t \sim \tau_\alpha$

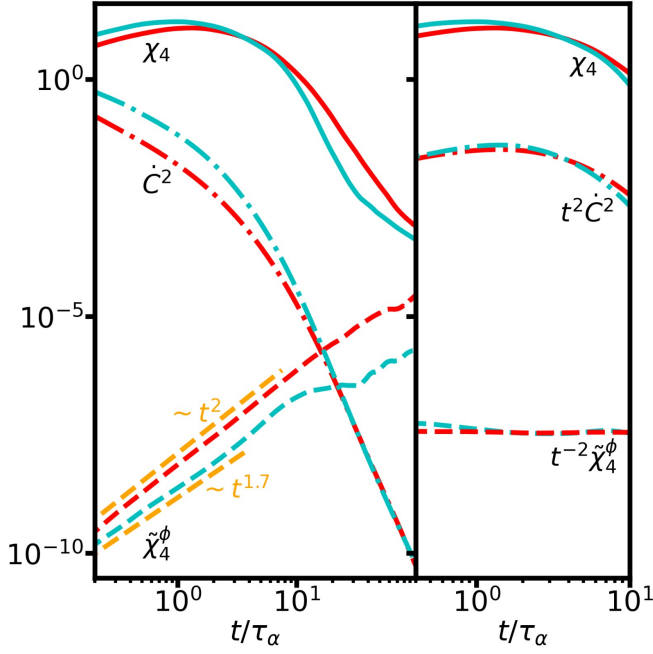


FIG. 2: Numerical results [17] for KALJ (cyan) and HARD (red). Left panel: $\chi_4(t)$ for KALJ for $T = 0.50$ and for HARD at $\phi = 0.58$, $10^6 \dot{C}^2(t)$ for KALJ at $T = 0.50$ and $10^{10} \dot{C}^2(t)$ for HARD at $\phi = 0.58$, $10^{-21} \tilde{\chi}_4^\phi(t)$ [22] for HARD at $\phi = 0.58$, and $10^{-17} \tilde{\chi}_4^\phi(t)$ for KALJ at $T = 0.50$. $\tilde{\chi}_4^\phi(t)$ is extracted from the data by $\tilde{\chi}_4^\phi(t) = [\chi_4(t) - \chi_{4,b}^{(0)}(t)] \dot{C}^{-2}(t)$. The yellow dashed lines represent a $\propto t^2$ time dependence (frozen heterogeneity approximation for $\tilde{\chi}_4^\phi(t)$), and a $\propto t^{1.7}$ time dependence. Right panel: $\chi_4(t)$ for KALJ at $T = 0.50$ and for HARD at $\phi = 0.58$, $t^2 \dot{C}^2(t)$ for KALJ at $T = 0.50$ and for HARD at $\phi = 0.58$, $10^{-10} t^{-2} \tilde{\chi}_4^\phi(t)$ for HARD at $\phi = 0.58$ and for KALJ at $T = 0.50$.

(Fig. 2). Initially, $\chi_4(t)$ grows rapidly due to the rapid growth of $\tilde{\chi}_4^\phi(t)$, but this growth gets cut off by the sharp decrease of $\dot{C}^2(t)$ near $t \sim \tau_\alpha$, corresponding to the fact that τ_α is the characteristic time for the decay of $C(t)$. This leads to $\chi_4(t)$ having its peak for $t \sim \tau_\alpha$ [11, 14], even if the exchange time is much longer [23]. Another way of looking at this is to rewrite $\dot{C}^2(t) \tilde{\chi}_4^\phi(t) = [t^2 \dot{C}^2(t)] [t^{-2} \tilde{\chi}_4^\phi(t)]$, where $t^{-2} \tilde{\chi}_4^\phi(t)$ is still featureless for $t \sim \tau_\alpha$ (Fig. 2), but $t^2 \dot{C}^2(t)$ has a peak at $t \sim \tau_\alpha$, which leads to the peak in $\chi_4(t)$. $\tilde{\chi}_4^\phi(t)$ controls the height of the peak of $\chi_4(t)$, and provides an overall measure of the heterogeneity, because it is approximately proportional to the mean quadratic drift $\langle [\Delta \phi_{\vec{r}}(t) - \langle \Delta \phi_{\vec{r}}(t) \rangle]^2 \rangle = \langle [\int_0^t \delta \gamma(\vec{r}, t')]^2 \rangle = \int_0^t dt'' \int_0^t dt' \chi_2^\phi(t'' - t')$ of the local clocks,

$$\tilde{\chi}_4^\phi(t) \equiv \rho \tau^2 \int_0^t dt'' \int_0^t dt' \tilde{\chi}_2^\phi(t'' - t'), \quad \text{with} \quad (15)$$

$$\tilde{\chi}_2^\phi(t) \equiv \chi_2^\phi(t) + \lim_{q \rightarrow 0} \rho^{-1} \{ [S_c(\cdot) - 1] * s(\cdot, t) \}(\vec{q}), \quad (16)$$

where $S_c(\vec{q}) \equiv [S(\vec{q}) - \rho \delta_{\vec{q},0}]$ is the connected part of the static structure factor and $f * g$ denotes a convolution. In fact, in most cases, $\tilde{\chi}_2^\phi(t) \approx \chi_2^\phi(t)$ [22].

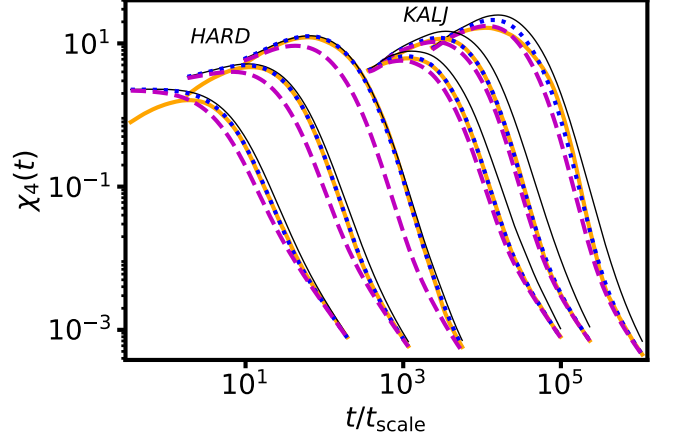


FIG. 3: Comparison of our model's predictions for $\chi_4(t)$, Eqs. (13)-(15), with numerical simulation results [17] (orange full lines) for: HARD for packing fractions $\phi = 0.55, 0.57, 0.58$ (left side, left to right) and KALJ for temperatures $T = 0.60, 0.55, 0.50$ (right side, left to right). t_{scale} is 1 for HARD and 0.065 for KALJ. Model predictions are shown for: (i) the frozen heterogeneity approximation $\chi_4(t) = \chi_{4,\text{fb}}(t)$ (black thin lines); (ii) $\tilde{\chi}_2^\phi(t) = \tilde{\chi}_2^\phi(0) e^{-t/\tilde{\tau}_{\text{ex}}}$ with $\tilde{\tau}_{\text{ex}} = \tau_\alpha$ [22] (magenta dashed lines); and (iii) $\tilde{\chi}_2^\phi(t) = \tilde{\chi}_2^\phi(0) e^{-t/\tilde{\tau}_{\text{ex}}}$ with $\tilde{\tau}_{\text{ex}}$ chosen by fitting the data with Eq. (19) (blue dotted lines).

Results: Upper bound for $\chi_4(t)$ and frozen heterogeneity approximation. Eqs. (13) and (15) imply there is an upper bound $\chi_{4,\text{fb}}(t)$ for $\chi_4(t)$,

$$\chi_4(t) \leq \chi_{4,\text{fb}}(t) \equiv \tilde{a}_\phi t^2 \dot{C}^2(t) + \chi_{4,b}^{(0)}(t), \quad \text{with} \quad (17)$$

$$\tilde{a}_\phi \equiv \rho \tau^2 \tilde{\chi}_{2,M} \quad \text{and} \quad \tilde{\chi}_{2,M} \equiv \sup_t \tilde{\chi}_2^\phi(t) < \infty, \quad (18)$$

where the parameter \tilde{a}_ϕ [22] represents the overall strength of the heterogeneity.

For times $\tau_\alpha \lesssim t \ll \tau_{\text{ex}}$, most slow (fast) regions will stay slow (fast), so that each of their local clock drifts $\int_0^t \delta \gamma(\vec{r}, t')$ will grow linearly with time. Thus for $\tau_\alpha \lesssim t \ll \tau_{\text{ex}}$, $\tilde{\chi}_4^\phi(t) \propto \langle (\text{local clock drift})^2 \rangle \propto t^2$. (Fig. 2 shows that this regime can be found for HARD but not for KALJ.) Equivalently, for $0 < t' < t \ll \tau_{\text{ex}}$, $\tilde{\chi}_2^\phi(t') \approx \tilde{\chi}_{2,M}$ [22]. Thus Eq. (17) becomes an approximate equality, $\chi_4(t) \approx \chi_{4,\text{fb}}(t)$. We refer to this as the *frozen heterogeneity approximation*. In this approximation, the time dependence of the dynamic susceptibility $\chi_4(t)$ is given by an explicit expression in terms of independently measured quantities – $C(t)$ and $\langle (\delta N)^2 \rangle$ – plus a single numerical constant, \tilde{a}_ϕ .

By contrast, for $t \gtrsim \tau_{\text{ex}}$ the inequality in Eq. (17) becomes strict. For $t \gg \tau_{\text{ex}}$, a given region will pass through periods in which it is slow and periods in which it is fast, so local drifts will alternate between positive and negative signs, and $\tilde{\chi}_4^\phi(t) \propto \langle (\text{local clock drift})^2 \rangle \ll (\text{const}) t^2$. In particular, if $\tilde{\chi}_2^\phi(t)$ decays like $t^{-1-\delta}$ ($\delta > 0$) or faster, then $\tilde{\chi}_4^\phi(t) \propto t \ll t^2$.

Fig. 3 shows a comparison of our model's predictions

for $\chi_4(t)$ with numerical results [17] for HARD and KALJ. To explore the effects of the exchange time on the results, we choose the simple parametrization $\tilde{\chi}_2^\phi(t) = \tilde{\chi}_2^\phi(0)e^{-t/\tilde{\tau}_{\text{ex}}}$, which by Eq. (15) gives

$$\tilde{\chi}_4^\phi(t) = \tilde{a}_\phi \{2\tilde{\tau}_{\text{ex}}^2 [\exp(-t/\tilde{\tau}_{\text{ex}}) - 1 + t/\tilde{\tau}_{\text{ex}}]\}. \quad (19)$$

There is a narrow band of possible results of the model between the cases of frozen heterogeneity [$\tilde{\tau}_{\text{ex}} = \infty, \chi_4(t) = \chi_{4,\text{fh}}(t)$] and of $\tilde{\tau}_{\text{ex}} = \tau_\alpha$. The numerical results fall within that range for $t \gtrsim \tau_\alpha$ for HARD at $\phi = 0.55, 0.57$ and for $t \gtrsim 0.1\tau_\alpha$ for all other cases [16]. For HARD they approach the frozen heterogeneity upper bound $\chi_{4,\text{fh}}(t)$ as the packing fraction increases. For KALJ, they are closer to the $\tau_{\text{ex}} = \tau_\alpha$ results. In fact, remarkable agreement can be obtained if the form in Eq. (19) is used, with $\tilde{\tau}_{\text{ex}}$ as a fitting parameter. (For KALJ at $T = 0.50$, the data are too noisy to judge on goodness of fit.)

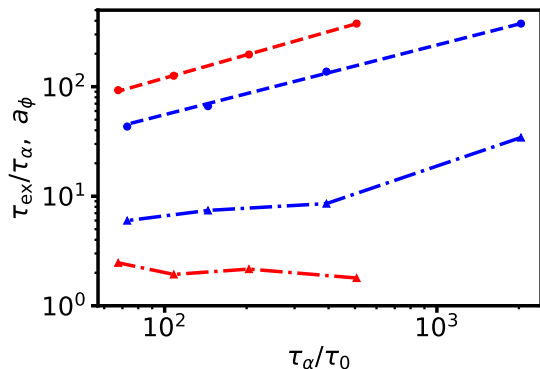


FIG. 4: Ratio $Q = \tau_{\text{ex}}/\tau_\alpha$ (triangles) and heterogeneity strength parameter a_ϕ (circles), vs rescaled relaxation time τ_α/τ_0 ([10]), for HARD (blue) at $\phi = 0.55, 0.56, 0.57, 0.58$ and KALJ (red) at $T = 0.70, 0.65, 0.60, 0.55$. The dashed lines are power law fits for a_ϕ .

Results: Exchange time τ_{ex} Fig. 4 shows initial estimates of the memory parameter $Q \equiv \tau_{\text{ex}}/\tau_\alpha$ [7] and the heterogeneity strength parameter a_ϕ , obtained under the assumption that $\chi_2^\phi(t) = \chi_2^\phi(0)e^{-t/\tau_{\text{ex}}}$, which corresponds to $\chi_4(t) = \dot{C}^2(t)a_\phi \{2\tau_{\text{ex}}^2 [\exp(-t/\tau_{\text{ex}}) - 1 + t/\tau_{\text{ex}}]\} + \chi_{4,b}(t)$ [16]. For KALJ $Q \sim 2$ and it seems not to vary strongly with τ_α [23], but for HARD, Q increases from ~ 5 to $\gtrsim 30$ as the glass transition is approached. For both models, $a_\phi \sim \tau_\alpha^p$, with $p_{\text{HARD}} \approx 0.64$ and $p_{\text{KALJ}} \approx 0.70$.

Summary. We have introduced a simple phenomenological model for dynamic heterogeneity in glass-forming materials. This model translates into quantitative predictions the intuitive description of dynamic heterogeneities as local fluctuations in the relaxation rate, and additionally takes into account contributions due to local particle density fluctuations and to single-particle, non-collective behavior.

The model provides expressions for computing four-point functions - such as Eqs. (13)-(16) - requiring only one- and

two-point quantities - like ρ , $S(\vec{q})$, $C(t)$, and the relaxation rate two-point correlation function $s(\vec{q}, t)$ - that are much easier to interpret than four-point functions. Crucially, Eq. (13), shows that $\chi_4(t)$ having a peak at $t \sim \tau_\alpha$ is due to $\dot{C}^2(t)$ having its characteristic time at $t \sim \tau_\alpha$, even though $\tilde{\chi}_4^\phi(t)$ is the factor that most directly encodes the time dependence of relaxation rate fluctuations. This explains why the lifetime of the dynamic heterogeneities has a weak effect on the location $t = t_4 \sim \tau_\alpha$ of the peak of $\chi_4(t)$.

Given a single parameter \tilde{a}_ϕ encoding the overall strength of the relaxation rate fluctuations, the model predicts an upper bound $\chi_{4,\text{fh}}(t)$ for the dynamic susceptibility $\chi_4(t)$, corresponding to the limit of frozen heterogeneity, $\tilde{\tau}_{\text{ex}} = \infty$. If, additionally, it is assumed that the two-point susceptibility decays exponentially, $\tilde{\chi}_2^\phi(t) = \tilde{\chi}_2^\phi(0)e^{-t/\tilde{\tau}_{\text{ex}}}$, very good agreement is obtained with numerical data by fitting with the two parameters $\tilde{a}_\phi, \tilde{\tau}_{\text{ex}}$. The dependence of $\chi_4(t)$ on $\tilde{\tau}_{\text{ex}}$ is relatively weak, and all numerical data fall in the narrow interval between the $\tilde{\tau}_{\text{ex}} = \tau_\alpha$ prediction and the frozen heterogeneity $\tilde{\tau}_{\text{ex}} = \infty, \chi_4(t) = \chi_{4,\text{fh}}(t)$ prediction.

Information about the time evolution of the heterogeneities can be found most clearly in the time evolution of $\chi_4(t)$ after its peak. Roughly speaking, $\tau_{\text{ex}} = \infty$ makes the heterogeneities maximally persistent, which maximizes the strength of the heterogeneity, i.e. $\chi_4(t) \approx \chi_{4,\text{fh}}(t)$, but the shorter τ_{ex} is, the faster the heterogeneous relaxation rates return to the mean, and the more $\chi_4(t)$ differs from $\chi_{4,\text{fh}}(t)$ for times $t \gtrsim \tau_{\text{ex}}$. Estimating $Q = \tau_{\text{ex}}/\tau_\alpha$ from $\chi_4(t)$ shows that $Q_{\text{KALJ}} \sim 2$ independently of τ_α [23], but Q_{HARD} grows strongly with τ_α . (We believe this to be the first measurement of Q or τ_{ex} for a hard sphere model.) These results are consistent with the fact that for HARD at higher packing fraction (but not for KALJ), there is a time regime $\tau_\alpha \lesssim t \ll \tau_{\text{ex}}$ where the frozen heterogeneity approximation holds, i.e. $\tilde{\chi}_4^\phi(t) \sim t^2$ (Fig. 2) and $\chi_4(t) \approx \chi_{4,\text{fh}}(t)$ (Fig. 3).

Finally, the model introduces $s(\vec{q}, t)$, which quantifies more directly the spatial and temporal correlations of the local relaxation rate. Results for this quantity, plus discussions of non-TTI dynamics, more general overlap functions $w_n(t)$, four-point functions with general time arguments, and connections to experimentally measured correlators [4, 6–8], will be reported elsewhere [24, 25].

Acknowledgements We thank Elijah Flenner for providing the numerical simulation data that was analyzed in this work. R. K. P. acknowledges the Ohio University Condensed Matter and Surface Sciences (CMSS) program for support through a studentship.

† castillh@ohio.edu

- [1] E. Donth, *The Glass Transition* (2001) p. 432.
- [2] C. A. Angell, K. L. Ngai, G. B. McKenna, P. F. McMillan, and S. W. Martin, *Journal of Applied Physics* **88**, 3113 (2000).
- [3] P. G. Debenedetti and H. Stillinger Frank, *Nature* **410**, 259

- (2001).
- [4] M. D. Ediger, *Annual Review of Physical Chemistry* **51**, 99 (2000).
- [5] L. Berthier, G. Biroli, J.-P. Bouchaud, L. Cipelletti, and W. van Saarloos, eds., *Dynamical Heterogeneities in Glasses, Colloids, and Granular Media* (Oxford University Press, 2011).
- [6] H. Sillescu, *Journal of Non-Crystalline Solids* **243**, 81 (1999).
- [7] R. Richert, *Proceedings of the National Academy of Sciences* **112**, 4841 (2015).
- [8] K. Paeng, H. Park, D. T. Hoang, and L. J. Kaufman, *Proceedings of the National Academy of Sciences* **112**, 4952 (2015).
- [9] E. Flenner, M. Zhang, and G. Szamel, *Physical Review E* **83**, 051501 (2011).
- [10] E. Flenner, H. Staley, and G. Szamel, *Physical Review Letters* **112**, 097801 (2014).
- [11] N. Lačević, F. W. Starr, T. B. Schröder, and S. C. Glotzer, *The Journal of Chemical Physics* **119**, 7372 (2003).
- [12] C. Dasgupta, A. V. Indrani, S. Ramaswamy, and M. K. Phani, *Europhysics Letters (EPL)* **15**, 307 (1991).
- [13] L. Berthier and G. Biroli, *Reviews of Modern Physics* **83**, 587 (2011).
- [14] C. Toninelli, M. Wyart, L. Berthier, G. Biroli, and J.-P. Bouchaud, *Physical Review E* **71**, 041505 (2005).
- [15] A. Parsaeian and H. E. Castillo, *Physical Review E* **78**, 060105 (2008).
- [16] (). See Supplemental Material for additional details.
- [17] Ohio Supercomputer Center, “Ohio Supercomputer Center, <http://osc.edu/ark:/19495/f5s1ph73>,” (1987).
- [18] R. K. Pandit, E. Flenner, and H. E. Castillo, *Physical Review E* **105**, 014605 (2022).
- [19] G. A. Mavimbela, A. Parsaeian, and H. E. Castillo, Preprint arXiv:1210.1249 (2012).
- [20] G. A. Mavimbela, A. Parsaeian, and H. E. Castillo, *AIP Advances* **9**, 015210 (2019).
- [21] R. K. Pandit, *Local Fluctuations in the Relaxation Rate in Glassy Systems*, Ph.D. thesis, Ohio University (2019).
- [22] (), The $\tilde{\chi}$ symbol identifies five quantities, i.e. $\tilde{\chi}_4^\phi(t)$, $\tilde{\chi}_2^\phi(t)$, $\tilde{\chi}_{2,M}$, $\tilde{\tau}_{ex}$ and \tilde{a}_ϕ , that mostly quantify relaxation rate fluctuations but contain a small correction from density fluctuations. (See Supplemental Material for additional details.).
- [23] K. Kim and S. Saito, *The Journal of Chemical Physics* **138**, 12A506 (2013).
- [24] R. K. Pandit and H. E. Castillo, manuscript in preparation (2023).
- [25] H. E. Castillo and R. K. Pandit, manuscript in preparation (2023).

Supplemental Material for: A simple model for dynamic heterogeneity in glass-forming liquids

Rajib K Pandit* and Horacio E. Castillo[†]

Department of Physics and Astronomy and Nanoscale and Quantum Phenomena Institute, Ohio University, Athens, Ohio 45701, USA
(Dated: October 24, 2023)

Numerical data and data analysis We analyze numerical simulation data for two 3D equilibrium glass-forming liquids. The first is a set of Monte Carlo simulations of a 50:50 binary mixture of $N = 80000$ hard-spheres (HARD), with diameters d and $1.4d$, at packing fractions $\varphi = 0.50, 0.52, 0.55, 0.56, 0.57$, and 0.58 [1]. The second is a set of Newtonian dynamics simulations of an $N = 27000$ Kob-Andersen Lennard-Jones (KALJ) [2–4] system, at a density $\rho = N/V = 1.2$, with temperatures $T = 0.50, 0.55, 0.60, 0.65, 0.70$, and 0.80 [5]. More details on the simulations can be found in Ref. [1] for HARD and in Ref. [5] for KALJ.

To obtain $\chi_4(t)$, we fitted [6] $S_4(\vec{q}, t)$ with the form [7]

$$S_4(\vec{q}, t) = \frac{\chi_4^{\text{cr}}(t)}{1 + [\xi_4^{\text{cr}}(t)]^2 q^2 + [c(t)]^2 q^4} + \chi_{4,b}(t), \quad (1)$$

where $\chi_4^{\text{cr}}(t)$ is the collective relaxation part of the dynamic susceptibility, $\xi_4^{\text{cr}}(t)$ is the four-point dynamic correlation length, and $\chi_4(t) = \chi_4^{\text{cr}}(t) + \chi_{4,b}(t)$. For t long enough that Eq. (12) in the main text is expected to be accurate [8], we extract [6]

$$\tilde{\chi}_4^\phi(t) = [\chi_4(t) - \chi_{4,b}^{(0)}(t)] \dot{C}^{-2}(t), \quad \text{and} \quad \tilde{a}_\phi = \lim_{t \rightarrow 0} t^{-2} \tilde{\chi}_4^\phi(t). \quad (2)$$

Range of validity of the approximations shown in Fig. 3 in the main text A likely explanation for the fact that the model starts to represent well the data at earlier t/τ_α fractions in some cases is that for the glassier cases, there is a stronger separation between the timescales of the first and second step in the two-step relaxation, which makes Eq. (12) in the main text - and consequently Eqs. (13) and (17) in the main text - accurate over a wider range of timescales, and in particular even for times shorter than τ_α .

$S_4^{\text{mc}}(\vec{q}, t)$, and the relations between $\tilde{\chi}_2^\phi(t)$ and $\chi_2^\phi(t)$, and between $\tilde{\tau}_{\text{ex}}$ and τ_{ex} . $\tilde{\tau}_{\text{ex}}$ characterizes the decay with time of $\tilde{\chi}_2^\phi(t)$ [Eq. (16)], which incorporates a correction to $\chi_2^\phi(t)$ [Eq. (10)] due to the interplay of density and relaxation rate fluctuations. It differs slightly from τ_{ex} , which characterizes only the relaxation rate fluctuations probed by $\chi_2^\phi(t)$, as shown in Fig. SM-1.

In the case of $\tilde{\tau}_{\text{ex}}$, combining Eqs. (13) and (19) in the main text leads to

$$\chi_4(t) = \dot{C}^2(t) \tilde{a}_\phi \{2\tilde{\tau}_{\text{ex}}^2 [\exp(-t/\tilde{\tau}_{\text{ex}}) - 1 + t/\tilde{\tau}_{\text{ex}}]\} + \chi_{4,b}^{(0)}(t). \quad (3)$$

Here the background value $\chi_{4,b}^{(0)}(t)$ is separately determined from $C(t)$ and $S(q)$ by using Eq. (14) in the main text.

In the case of τ_{ex} , we repeat the derivation that leads to Eq. (13) in the main text, but we collect terms in a slightly different way. Thus we obtain

$$\chi_4(t) \equiv \lim_{q \rightarrow 0} S_4(\vec{q}, t) = \dot{C}^2(t) \chi_4^\phi(t) + \chi_{4,b}(t), \quad \text{with} \quad (4)$$

$$\chi_4^\phi(t) \equiv \rho \tau^2 \int_0^t dt'' \int_0^t dt' \chi_2^\phi(t'' - t'), \quad (5)$$

$$\chi_{4,b}(t) \approx \chi_{4,b}^{(0)}(t) + \lim_{q \rightarrow 0} S_4^{\text{mc}}(\vec{q}, t), \quad \text{and} \quad (6)$$

$$S_4^{\text{mc}}(\vec{q}, t) = \dot{C}^2(t) \tau^2 \int_0^t dt'' \int_0^t dt' \{ [S_c(\cdot) - 1] * s(\cdot, t'' - t') \}(\vec{q}). \quad (7)$$

Here $\chi_2^\phi(t)$ and $s(\vec{q}, t)$ are defined in Eqs. (10) and (11) in the main text, $S_c(\vec{q}) \equiv [S(\vec{q}) - \rho \delta_{\vec{q},0}]$ is the connected part of the static structure factor and $f * g$ denotes a convolution. We notice that $\chi_{4,b}(t)$ is the same quantity that was defined in Ref. [7]. By assuming that $\chi_2^\phi(t) = \chi_2^\phi(0) e^{-t/\tau_{\text{ex}}}$, the equations above lead to

$$\chi_4(t) = \dot{C}^2(t) a_\phi \{2\tau_{\text{ex}}^2 [\exp(-t/\tau_{\text{ex}}) - 1 + t/\tau_{\text{ex}}]\} + \chi_{4,b}(t). \quad (8)$$

From the numerical point of view, we see that the difference between $\tilde{\chi}_2^\phi(t)$ (or $\tilde{\tau}_{\text{ex}}$) and $\chi_2^\phi(t)$ (or τ_{ex}) comes from

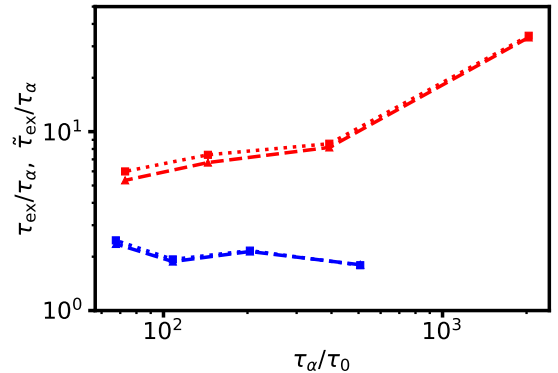


FIG. SM-1: Ratios $\tau_{\text{ex}}/\tau_\alpha$ (triangles) and $\tilde{\tau}_{\text{ex}}/\tau_\alpha$ (squares), as functions of the rescaled relaxation time τ_α/τ_0 ([5]) for HARD (blue) at $\varphi = 0.55, 0.56, 0.57, 0.58$ and KALJ (red) at $T = 0.70, 0.65, 0.60, 0.55$.

*Present address: Exact Sciences, Redwood City, 94063 CA, USA

the difference between the $\chi_{4,b}^{(0)}(t)$ background in the first case and the $\chi_{4,b}(t)$ background in the second. From the point of view of *predicting* the behavior of $\chi_4(t)$, the former is preferable because $\chi_{4,b}^{(0)}(t)$ is completely determined by the global average quantities $C(t)$ and $S(q)$, i.e. it does not require any prior information regarding dynamic heterogeneity. For this reason it is used in the analysis shown in Figs. 2 and 3 in the main text. By contrast, from the point of view of estimating the lifetime of heterogeneities, τ_{ex} is preferable to $\tilde{\tau}_{\text{ex}}$, because it is the same quantity defined in Eq. (10) in the main text, which does not include any extra contributions associated with density fluctuations, and for this reason τ_{ex} and a_ϕ are the quantities that are shown in Fig. 4 in the main text.

In practice, as pointed out in Ref. [7], the difference between $\chi_{4,b}(t)$ and $\chi_{4,b}^{(0)}(t)$ is very small. This implies that the difference between $\tilde{\chi}_2^\phi(t)$ and $\chi_2^\phi(t)$, and the difference between $\tilde{\tau}_{\text{ex}}$ and τ_{ex} are both small. In the case of the characteristic times, this is confirmed by the results shown in Fig. SM-

1.

† castillh@ohio.edu

- [1] E. Flenner, M. Zhang, and G. Szamel, *Physical Review E* **83**, 051501 (2011).
- [2] W. Kob and H. C. Andersen, *Physical Review Letters* **73**, 1376 (1994).
- [3] W. Kob and H. C. Andersen, *Physical Review E* **51**, 4626 (1995).
- [4] W. Kob and H. C. Andersen, *Physical Review E* **52**, 4134 (1995).
- [5] E. Flenner, H. Staley, and G. Szamel, *Physical Review Letters* **112**, 097801 (2014).
- [6] O. S. Center, “[Ohio supercomputer center](#),” (1987).
- [7] R. K. Pandit, E. Flenner, and H. E. Castillo, *Physical Review E* **105**, 1 (2022).
- [8] In particular the estimation of the limit $t \rightarrow 0$ for \tilde{a}_ϕ is an extrapolation where data are excluded for shorter times.